Journal of Physics: Conference Series **503** (2014) 012033 doi:10.1088/1742-6596/503/1/012033

Non-mesonic weak decay of hypernuclei with effective field theory

A Pérez-Obiol[1], D R Entem[2], B Juliá-Díaz[1,3] and A Parreño[1]

[1] Departament d'Estructura i Constituents de la Matèria,
Institut de Ciències del Cosmos (ICC),
Universitat de Barcelona, Martí i Franquès 1, E–08028 Barcelona, Spain
[2] Grupo de Física Nuclear and IUFFyM,
Universidad de Salamanca, E-37008 Salamanca, Spain
[3] ICFO - Institut de Ciències Fotòniques,
Av. Carl Friedrich Gauss 3, E–08860 Castelldefels (Barcelona), Spain

E-mail: axel@ecm.ub.edu, entem@usal.es, bruno@ecm.ub.edu, assum@ecm.ub.edu

Abstract. The $\Lambda N \to NN$ interaction, the main responsible for the decay of heavy hypernuclei, is described within the effective field theory (EFT) framework. The EFT is developed up to $\mathcal{O}(\vec{q}^{\,2})$, where $\vec{q}$ is the transferred momentum between the interacting baryons. Numerical values for the leading order low-energy constants are obtained by two means. First, from a fit to the hypernuclear decay observables, and second, by comparing the EFT to the one-meson-exchange model describing the same interaction. All the two-pion exchange diagrams entering at the next-to-leading in the EFT have been calculated.

1. Introduction

During the last 60 years hypernuclear experiments have helped us to understand how hyperons —baryons with strangeness— and nucleons interact, and how they form the bound states we call hypernuclei. Nowadays, a few tens of hypernuclei have been characterized (see Fig. 1), and in the coming years many more should be produced at experiments such as HypHI [1] and PANDA [2] at FAIR. The lightest hyperon, the Λ, has valence quarks u, d and s, a mass of ~ 1116 MeV, zero charge and zero isospin. It decays through the weak interaction in $\sim 2.6 \cdot 10^{-10}$ seconds, and hence it is very difficult to perform ΛN scattering experiments. Therefore, hypernuclei are the main laboratories to study ΛN interactions. On the one hand, the binding energies of these hypernuclei give us information about the nuclear structure and about the strong hyperon-nucleon forces. On the other hand, the decay of hypernuclei allows us to constrain the weak ΛN interaction.

The weak $\Lambda N \to NN$ transition is the main mechanism driving the decay of heavy hypernuclei. While in free space the Λ decays mostly to a nucleon and a pion, when it is embedded in $A > 5$ hypernuclei, this mechanism becomes highly suppressed. This effect is due to the Pauli-blocking of the nucleonic medium on the final nucleon. In contrast, the final nucleons in single-, $\Lambda N \to NN$, and multi-nucleon ($\Lambda NN \to NNN$, etc.) induced decay mechanisms have enough energy to either escape the nucleus or occupy states above the Fermi energy level.

The $\Delta S = 1$ ΛN interaction has been traditionally studied with one-meson-exchange models (OME) [4]. Within this picture, the different ranges of the potential are described by the

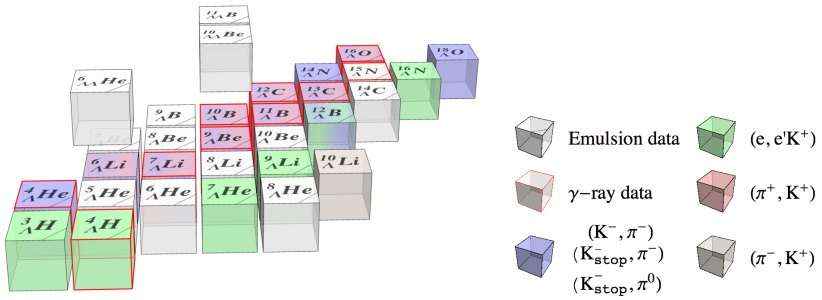

Figure 1. (Color online) Low mass region of layers $s = -1$ and $s = -2$ of the nuclear landscape. The different hypernuclei are colored according to the reactions that have produced them. In the coming years, new experiments will contribute with more hypernuclei in both layers. Original data for the Λ-hypernuclei is taken from [3].

exchange of the lightest pseudoscalar and vector mesons (π, K, η, ρ, ω and K^*). This model has been very useful to describe the hypernuclear decay data, but it is very model dependent and its connection to the underlying physics is difficult to establish. First, the non-pionic couplings and form factors are not experimentally known, and must be derived using $SU(3)$ flavor and $SU(6)$ flavor-spin symmetries, which are largely broken. Second, the heaviest mesons, which account for the short range part of the interaction, are too large to probe the physics at the ranges given by the corresponding Yukawa potentials.

In our work we describe the two-body weak $\Delta S = 1$ ΛN interaction within an effective field theory (EFT) framework, following the works of Refs. [5, 6]. The EFT approach allows one to study the baryon-baryon interactions in a more systematic and less model dependent way. The main idea is to separate a soft scale, which contains only the degrees of freedom that are relevant in the interaction (i.e. pions and kaons) from a hard scale (of the order of the mass of the nucleon). Then, one constructs the potential only with these degrees of freedom while respecting the symmetries of the underlying theory, as for example, chiral symmetry. The potential is built as an expansion on a parameter which is a ratio of the low scale over the hard scale. In baryon-baryon interactions, this expansion parameter is usually the transferred momentum between the baryons over the average mass of the baryons. To organize this expansion, we use the Weinberg power counting scheme [7] and the heavy baryon expansion [8].

The description for the $\Lambda N \to NN$ interaction is constrained by the value of the hypernuclear decay observables. When a hypernucleus decays non-mesonically, we can observe, mainly, three different quantities: the total non-mesonic decay rate, Γ_{nm}; the partial decay rates, $\Gamma_n = \Gamma(\Lambda n \to nn)$ and $\Gamma_p = \Gamma(\Lambda p \to np)$, with $\Gamma_{nm} = \Gamma_n + \Gamma_p$; and the asymmetry in the distribution of protons coming from the decay of polarized hypernuclei.

2. Leading order Effective field theory

The leading order (LO) EFT for the $\Lambda N \to NN$ interaction involves the long-ranged one-pion exchange (OPE), the medium-long ranged one-kaon exchange (OKE), and two contact operational structures. The Feynman diagrams for these contributions are depicted in Fig. 2. The kaon is included as an explicit degree of freedom since its mass (~ 495 MeV) is comparable to the momentum transferred to the final baryons (~ 400 MeV).

The strong vertex $NN\pi$ and the weak $\Lambda N\pi$ one are experimentally known from the corresponding decays. The kaon vertices, however, are not available experimentally, and one needs to use $SU(3)$ symmetry to relate them to the pionic ones. We use the values given by the Nijmegen Soft-Core 97 f [9] and the Jülich B [10] models.

The contact potential is made up of all the possible operational structures that connect initial and final spin, isospin and angular momentum states. Taking into account the antisymmetry of the final nucleons, and at zeroth order in the momentum expansion, we have two independent

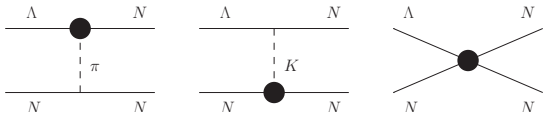

Figure 2. One-pion exchange, one-kaon exchange and contact contributions to the transition. The solid circle represents the weak interaction vertex.

structures:

$$V_{4P}(\vec{q}) = C_{00} + C_{01}\ \vec{\sigma}_1\vec{\sigma}_2\,. \tag{1}$$

The two low-energy constants (LEC's) appearing in the contact potential are not known and must be fitted to the experiment. Therefore, we need to relate the two-body transition to the hypernuclear decay rate, which involves the knowledge of the initial and final many-body states. For the initial state we use a shell model approach, and assume that the Λ is coupled to the lowest energy level. To uncouple a nucleon from the core we use the technique of the coefficients of fractional parentage. The interacting Λ and nucleon are described by harmonic oscillator wave functions, with the parameters b_N and b_Λ such that the core and hypernucleus binding energies are reproduced, respectively. Regarding the final wave function, we have not included the propagation of the two primary outgoing nucleons within the residual medium. In our approximation, the residual $(A-2)$ nucleus acts as a spectator, and only the strong interaction among these two primary nucleons is considered. More specifically, we solve a Lippmann-Schwinger scattering equation with the input of modern potential models (Nijmegen Soft-Core 97 f and Jülich B).

We have fitted the low-energy constants to reproduce the experimental data for three different hypernuclear observables and for three different hypernuclei — ${}^{5}_{\Lambda}He$, ${}^{11}_{\Lambda}B$ and ${}^{12}_{\Lambda}C$ —. In Fig. 3 we show the experimental data points together with the results obtained from this fit. We obtain two sets of data points, one for each of the two models used in the strong part of the calculation. The results obtained from the Jülich model fit a little better the data, but both models show that the data is fairly well reproduced by a LO EFT [11].

An alternative way to obtain information about the LEC's is to compare the EFT description with the OME one. In both formalisms the long and medium range is described by the one-pion and one-kaon exchanges, therefore we only need to match the short range terms in both formalisms. While in the EFT the operational structures are already organized in powers of momentum, the heavy meson exchange potentials in the OME approach are not. To obtain these different operational structures, we expand the OME potentials in powers of $\frac{q}{m}$ and $\frac{q}{\Lambda}$,

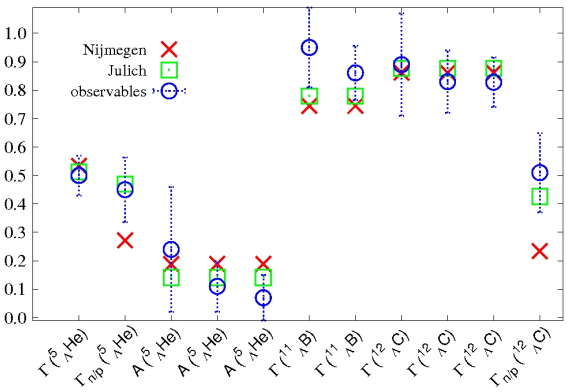

Figure 3. Hypernuclear decay observables (total and partial decay rates and asymmetry for ${}^{\Lambda}_{5}$He, ${}^{\Lambda}_{11}$B and ${}^{\Lambda}_{12}$C), including their error bars and their fitted values. The total decay rates are in units of the Λ decay rate in free space ($\Gamma_\Lambda = 3.8\times10^{9}\mathrm{s}^{-1}$). All the quantities are adimensional.

	Nijmegen		Jülich	
	OME expansion	LO PC calculation	OME expansion	LO PC calculation
C_0^0	1.07 ± 0.88	(4.01 ± 0.23)	-1.7 ± 2.6	(4.03 ± 0.50)
C_0^1	0.02 ± 0.36	(0.02 ± 0.33)	0.12 ± 0.37	(-0.30 ± 0.28)

Table 1. Values for the LEC's obtained from the two sources: OME expansion and LO (PC) EFT calculation, using the Nijmegen and Jülich strong interaction models. All the quantities are in units of $G_F = 1.166 \times 10^{-11}$ MeV^{-2}.

where m and Λ are the meson mass and cut-off used in the applicable potential. Thus, we can write the LEC's appearing in the LO EFT in terms of the heavy meson parameters. This way of assigning values to the LEC's is called resonance saturation and it has been previously applied in the strong NN case [12].

In Table 1 the values obtained for the LEC's according to each approach and for each model are shown. The larger discrepancy is found to affect the LEC C_{00}. This partly motivated us to include a sigma meson in the OME picture and to study how it affects the numerical values of LEC's. When the potential for the isoscalar sigma meson is expanded, and then included in the resonance saturation study, the LEC C_{01} stays the same while the LEC C_{00} has an extra term that depends linearly on the unknown parity-violating $\Lambda N\sigma$ coupling, A_σ. Thus, we can use this procedure to set bounds on the values of A_σ. For example, taking the values of $m_\sigma = 550$ MeV and $g_{NN\sigma} = 8.8$ from Ref. [13], and working within the Nijmegen strong potential model, we find $3.3 \leq A_\sigma \leq 7.3$ [11].

3. Next-to-leading order

The following order in the EFT includes all the possible operational structures at orders $\mathcal{O}(|\vec{q}|)$ and $\mathcal{O}(\vec{q}^2)$ and the contributions coming from the two-pion exchange diagrams. In total we have 13 independent operational structures, and therefore 13 LEC's that, in principle, should be fitted to the experiment. However, this is not feasible with the current hypernuclear experimental data. One way to reduce this number of LEC's is to neglect the initial momentum (of the order of a few tens of MeV) in front of the final one (of the order of 400 MeV). Within this approximation, the contact potential at $\mathcal{O}(|\vec{q}|)$ and $\mathcal{O}(\vec{q}^2)$ contains only 6 LEC's and reads (in units of G_F):

$$V_{4P}(\vec{q}) = C_{10}\,\frac{\vec{\sigma}_1\vec{q}}{2M_N} + C_{11}\,\frac{\vec{\sigma}_2\vec{q}}{2M_N} + \mathrm{i}\,C_{12}\,\frac{(\vec{\sigma}_1\times\vec{\sigma}_2)\,\vec{q}}{2M_N} + C_{20}\,\frac{\vec{\sigma}_1\vec{q}\,\vec{\sigma}_2\vec{q}}{4M_N^2} + C_{21}\,\frac{\vec{\sigma}_1\vec{\sigma}_2\,\vec{q}^{\,2}}{4M_N^2} + C_{22}\,\frac{\vec{q}^{\,2}}{4M_N^2}\,.$$

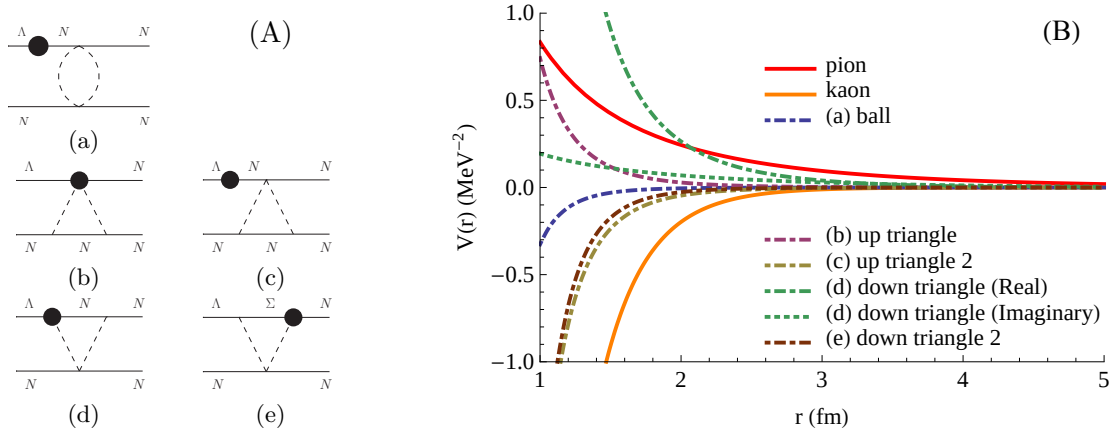

Figure 4. (Color online) (A) Feynman diagrams for the ball and triangle diagrams contributing to the $\Lambda N \to NN$ interaction. (B) Medium-long range part of the potentials for the one-pion-exchange, one-kaon-exchange, ball diagram and triangle diagrams

The two-pion exchange diagrams can be organized according to their topologies: balls, triangles and boxes. The momenta carried by the baryons in the loops of these diagrams are not constrained by any external momenta, and all their possible values must be integrated. These integrals have been calculated using dimensional regularization, with the minimal substraction scheme. Additionally, the two-pion exchange contributions involve the Σ hyperon as an explicit degree of freedom. The $\Sigma N\pi$ vertex is experimentally known from the weak decay of the Σ. The other vertices that appear in the loop diagrams and are not present in the one-meson exchanges, such as $\Lambda N\pi\pi$, are derived from the $SU(3)$ chiral Lagrangian. Full details of this calculation can be found in Ref. [14]. As a sample, the ball and triangle diagrams are depicted in Fig. 4 (A), and their potentials driving the ${}^3S_1 \to {}^3S_1$ transition are compared to the corresponding ones for the OPE and the OKE in Fig. 4 (B). At medium-long range, the two-pion exchange diagrams are comparable to the OPE and OKE mechanisms. However, they decay much faster than the OPE, which is the main contribution at long range.

4. Summary and perspectives

We have developed an EFT for the weak $\Lambda N \to NN$ transition up to $\mathcal{O}(\vec{q}^2)$. The numerical values for the LO LEC's have been obtained by two means. First, by a fit to the experimental data on the decay of hypernuclei, and second, by a comparison to the OME model describing the same interaction. Additionally, we have studied the possible inclusion of a σ meson in the OME picture, extracting thus a range for corresponding PV coupling. The next-to-leading order part of the EFT has been derived by systematically including all the possible two-pion exchange diagrams and operational structures up to second order in the momentum expansion.

In the future, we plan to reduce the model dependency of our approach by also using the EFT formalism in the strong sector. This is feasible for $A = 3, 4$ hypernuclei, where the few-body initial and final states can be solved using the Faddeev-Yakubovsky scheme [15]. Currently we are describing the non-mesonic decay of the hypertriton with our LO EFT weak potential and by using strong EFT potentials in both the initial hypernuclear wave function and the final state interactions. Once this calculation is completed, it can be easily extended to $A = 4$ hypernuclei.

Acknowledgments

This work is partly supported by grants FPA2010-21750-C02-02, FIS2008-00784 TOQATA and FIS2011-24154 from MICINN, 283286 from European Community-Research Infrastructure Integrating Activity 'Study of Strongly Interacting Matter', CSD2007-00042 from Spanish Ingenio-Consolider 2010 Program CPAN, and 2009SGR-1289 from Generalitat de Catalunya. A.P-O. acknowledges support by the APIF Ph.D. program of the University of Barcelona. B.J.D. is supported by the Ramon y Cajal program.

References

[1] T R Saito et al., Nucl. Phys. A **853**, 110 (2010).
[2] W Erni et al., Eur. Phys. J. A **49**, 25 (2013).
[3] O Hashimoto and H Tamura, Prog. Part. Nucl. Phys. **57**, 564 (2006).
[4] A Parreño, A Ramos, and C Bennhold, Phys. Rev. C **56**, 339 (1997).
[5] J-H Jun, Phys. Rev. C **63**, 044012 (2001).
[6] A Parreño, C Bennhold, and B R Holstein, Phys. Rev. C **70**, 051601 (2004); A Parreño, C Bennhold, and B R Holstein, Nucl. Phys. A **754**, 127c (2005).
[7] S Weinberg, Phys. Lett. B **251**, 288 (1990); S Weinberg, Nucl. Phys. B **363**, 3 (1991).
[8] E Jenkins and A Manohar, Phys. Lett. B **255**, 558-562 (1991).
[9] V G J Stoks and T A Rijken, Phys. Rev. C **59**, 3009 (1999); T A Rijken, V G J Stoks and Y Yamamoto, Phys. Rev. C **59**, 21 (1999).
[10] B Holzenkamp, K Holinde, and J Speth, Nucl. Phys. A **500**, 485 (1989).
[11] A Pérez-Obiol, A Parreño, and B Juliá-Díaz, Phys. Rev. C **84**, 024606 (2011).
[12] G Ecker, J Kambor, and D Wyler, Nucl. Phys. B **394**, 101 (1993).
[13] R Machleidt, Adv. Nucl. Phys. **19**, 189 (1989).
[14] A Pérez-Obiol, D R Entem, B Juliá-Díaz, and A Parreño, Phys. Rev. C **87**, 044614 (2013).
[15] H Kamada and W Glöckle, Nucl. Phys. A **548**, 205 (1992).